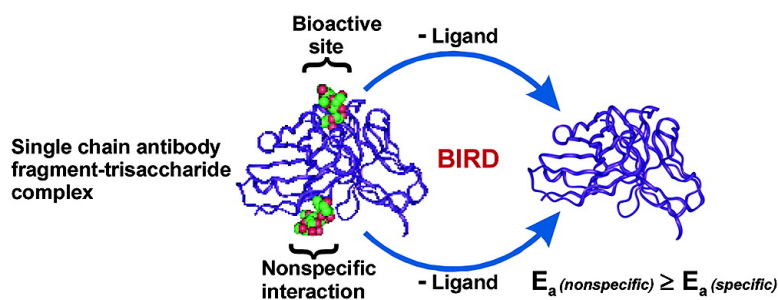


Bioactive Recognition Sites May Not Be Energetically Preferred in Protein–Carbohydrate Complexes in the Gas Phase

Weijie Wang, Elena N. Kitova, and John S. Klassen

J. Am. Chem. Soc., **2003**, 125 (45), 13630-13631 • DOI: 10.1021/ja036998q • Publication Date (Web): 16 October 2003

Downloaded from <http://pubs.acs.org> on March 30, 2009



More About This Article

Additional resources and features associated with this article are available within the HTML version:

- Supporting Information
- Links to the 3 articles that cite this article, as of the time of this article download
- Access to high resolution figures
- Links to articles and content related to this article
- Copyright permission to reproduce figures and/or text from this article

[View the Full Text HTML](#)



Bioactive Recognition Sites May Not Be Energetically Preferred in Protein–Carbohydrate Complexes in the Gas Phase

Weijie Wang, Elena N. Kitova, and John S. Klassen*

Department of Chemistry, University of Alberta, Edmonton, Alberta, Canada T6G 2G2

Received July 1, 2003; E-mail: john.klassen@ualberta.ca

Noncovalent solute–solute interactions and solvent effects govern affinity and specificity in biological recognition. Studies of desolvated biomolecular complexes may afford insight, hitherto unavailable, into their intrinsic binding affinity. To date, the limited structural studies of gaseous biomolecular complexes have focused primarily on the extent to which the structure of specific complexes, preformed in solution and transferred to the gas phase by electrospray (ES) or nanoES, is preserved.^{1,2} A related and as yet unexplored question is how the method of preparation influences the structure and stability of gaseous complexes. Here, we describe results from thermal dissociation experiments performed on gaseous protein–carbohydrate complexes originating from nonspecific interactions during the nanoES process. The stability of the nonspecific complexes as compared to the corresponding specific complex originating from interactions in solution provides the first evidence that a bioactive recognition site is not energetically preferred in the gas phase.

The carbohydrate-binding single chain fragment (scFv) of the monoclonal antibody Se155-4 and its native trisaccharide ligand, Gal α [Abe]Man (**1**),³ served as a model system for comparing the energetic and kinetic stability of a gaseous protein–ligand complex produced from specific interactions in solution and nonspecific interactions during the nanoES process. NanoES performed on an equimolar aqueous solution of scFv and **1** yields predominantly the protonated (scFv)^{*n*+} and (scFv + **1**)^{*n*+} ions, where *n* = 9–11. Using thermal dissociation experiments and functional group replacement, we have shown² that one of the specific intermolecular hydrogen bonds, His^{101H}–OH_{ManC4}, is preserved in the gaseous (scFv + **1**)^{*n*+} ions at *n* = 10. At *n* = 11, this specific hydrogen bond is absent. However, both the His^{101H} and the Man C-4 OH groups contribute to the stability of the complex.⁴ These results indicate that the specific interactions formed in solution impose constraints on the structure of the desolvated (scFv + **1**)^{*n*+} ions. At concentration ratios [1]/[scFv] \geq 2, (scFv + 2(**1**))^{*n*+} ions are also observed in the nanoES mass spectrum.⁵ Because the scFv has only a single binding site for **1**, the (scFv + 2(**1**))^{*n*+} ions must originate from nonspecific interactions between **1** and the specific scFv·**1** complex during the nanoES process. To distinguish these ligands, we will refer to them as specific (**1**_{sp}) or nonspecific (**1**_{ns}), that is, (scFv + 2(**1**))^{*n*+} \equiv (scFv + **1**_{sp} + **1**_{ns})^{*n*+}.

Time-resolved thermal dissociation experiments were performed on the gaseous, protonated (scFv + **1**)^{*n*+} and (scFv + 2(**1**))^{*n*+} ions, where *n* = 10, 11, produced by nanoES from solutions with [1]/[scFv] \geq 2, to evaluate the kinetic and energetic stability of the nonspecific complexes. The kinetic measurements were carried out using the blackbody infrared radiative dissociation (BIRD) technique⁶ implemented with a modified Fourier transform ion cyclotron resonance mass spectrometer.⁷

At temperatures of 120–165 °C, dissociation of the complexes proceeds exclusively by the loss of neutral **1**. In the case of the (scFv + 2(**1**))^{*n*+} ions, the sequential loss of **1** is observed. At both

charge states, plots of the natural log of the normalized abundance of the (scFv + 2(**1**))^{*n*+} ions versus reaction time are linear (Figure 1). Given that dissociation involves two parallel pathways (i.e., loss of **1**_{sp} or **1**_{ns}), the measured rate constant (*k*_{obs}) is equal to the sum of rate constants for the loss of the **1**_{sp} (*k*_{sp}) and **1**_{ns} (*k*_{ns}). The value of *k*_{ns} was determined from the measured *k*_{obs} and *k*_{sp}, which can be calculated at a given temperature from Arrhenius parameters for the dissociation of the (scFv + **1**_{sp})^{*n*+} ions.^{2b,c} In contrast, the natural log plots obtained for the dissociation of the (scFv + **1**)^{*n*+} ions, produced at [1]/[scFv] \geq 2, are nonlinear (Figure 1). The time dependence of the normalized abundance of the (scFv + **1**)^{*n*+} ions is reasonably described by a double exponential function, which incorporates *k*_{sp} (known) and *k*_{ns}. This result indicates that two distinct species are present, that is, (scFv + **1**_{sp})^{*n*+} and (scFv + **1**_{ns})^{*n*+}. Importantly, the values of *k*_{ns} determined at a given temperature with these two approaches are identical, within experimental error. This suggests that the nonspecific interactions are insensitive to the presence of **1**_{sp}. Arrhenius plots for the dissociation of the nonspecific protein–trisaccharide interactions were constructed from the temperature-dependent rate constants and are shown in Figure 2. Also included are the Arrhenius plots for the dissociation of the corresponding (scFv + **1**_{sp})^{*n*+} ions.^{2b,c} The Arrhenius activation energies and preexponential factors, *E*_a and *A*, are listed in Table 1.

The kinetic data obtained for the 1:1 and 1:2 complexes are consistent with the nonspecific ligand occupying a single site or, perhaps, several equivalent sites on the scFv. This result is surprising given that, by their very nature, nonspecific interactions are expected to lead to diverse structures. It may be that the nonspecific complexes relax to a common, lowest energy structure (or several equivalent structures) after or in concert with the desolvation process. Alternatively, only a fraction of the nonspecific complexes produced by nanoES, those that are most stable, may contribute to the kinetic measurements. Complexes with less favorable modes of binding will have shorter lifetimes and may dissociate in the ion source.

A comparison of the Arrhenius plots obtained for the dissociation of the specific and nonspecific complexes reveals that, over the temperature range investigated and at both charge states, the ions arising from nonspecific interactions are kinetically more stable (Figure 2). At the +11 charge state, the *E*_a's for the specific and nonspecific complexes are similar, 51–52 kcal/mol, and the greater kinetic stability of the nonspecific complex is entropic in origin. For the +10 ions, there is a striking difference in the *E*_a's, with the nonspecific complex being 7 kcal/mol more stable than the specific complex (61 versus 54 kcal/mol). It is also notable that the *E*_a for the +10 nonspecific complex is \sim 10 kcal/mol larger than that for the +11 species.

The enhanced energetic stability of the nonspecific +10 complex, as compared to the +10 specific complex, is surprising. A possible explanation for this observation is that, in addition to a number of

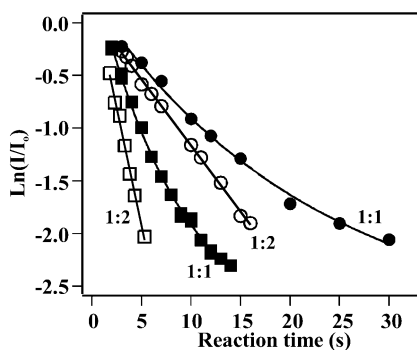


Figure 1. Plots of the natural logarithm of the normalized abundance (I/I_0) of the gaseous protonated complex ($(\text{scFv} + \mathbf{1})^{n+} \equiv 1:1$ (●, +10; ■, +11) and ($(\text{scFv} + 2(\mathbf{1}))^{n+} \equiv 1:2$ (○, +10; □, +11) ions versus reaction time measured at 142 °C.

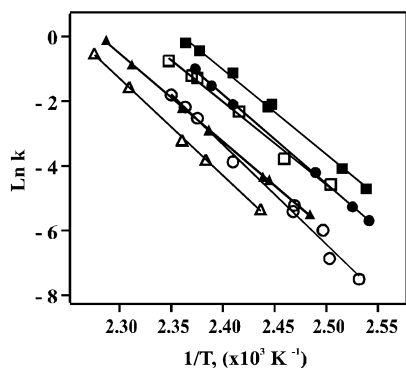


Figure 2. Arrhenius plots for the dissociation of the ($(\text{scFv} + \mathbf{1}_{\text{ns}})^{n+}$ (○, +10; □, +11), ($(\text{scFv} + \mathbf{1}_{\text{sp}})^{n+}$ (●, +10; ■, +11), and ($(\text{CA} + \mathbf{1})^{n+}$ (△, +10; ▲, +11) ions.

Table 1. Arrhenius Parameters Determined for the Dissociation of Gaseous, Protonated Protein–Trisaccharide Complexes: ($\text{P} + \text{L})^{n+} \rightarrow \text{P}^{n+} + \text{L}$

P	L	charge state	E_a^a (kcal/mol)	A^a (s^{-1})	$\Delta S^{\ddagger d}$ (cal/mol·K)
scFv	$\mathbf{1}_{\text{sp}}$	+10	54.3 ± 1.0^b	$10^{27.7 \pm 0.6 b}$	65
		+11	61.4 ± 2.4	$10^{30.8 \pm 1.3}$	80
	$\mathbf{1}_{\text{ns}}$	+10	52.1 ± 1.4^c	$10^{26.9 \pm 0.8 c}$	61
		+11	51.0 ± 2.3	$10^{25.9 \pm 1.2}$	57
CA	$\mathbf{1}$	+10	59.7 ± 1.1	$10^{29.5 \pm 0.5}$	74
		+11	54.0 ± 0.5	$10^{27.0 \pm 0.3}$	62

^a The reported errors are one standard deviation. ^b Arrhenius parameters taken from ref 2b. ^c Arrhenius parameters taken from ref 2c. ^d Values calculated at 415 K from the corresponding A-factors.

neutral hydrogen bonds, the ($(\text{scFv} + \mathbf{1}_{\text{ns}})^{10+}$ ion is stabilized by an ionic hydrogen bond involving one of the protonated scFv residues. Based on thermochemical data measured for the interaction between H_2O and protonated peptides, which is the best available model, solvation of a protonated scFv residue by one of the ligand OH groups can contribute as much as 15 kcal/mol to the stability of the complex.⁸ An alternative explanation lies in conformational constraints imposed by the specific interactions in solution, which may “trap” the complex, preventing it from adopting an optimal structure for hydrogen bonding in the gas phase. Such constraints are expected to be absent in the case of $\mathbf{1}_{\text{ns}}$, allowing for more favorable interactions in the gaseous complex. Regardless of the

nature of the interactions that stabilize the nonspecific +10 complex, the present results provide the first evidence that protein–ligand interactions remote from the bioactive recognition site can be energetically more favorable in the gas phase.

The propensity of $\mathbf{1}$ to form nonspecific interactions with proteins in the gas phase is further highlighted by the Arrhenius plots determined for the dissociation of the complex of bovine carbonic anhydrase II (CA) with $\mathbf{1}$ (Figure 2). CA, a Zn(II) metalloenzyme, does not interact specifically in solution with $\mathbf{1}$, and the gaseous $(\text{CA} + \mathbf{1})^{n+}$ ions result from nonspecific interactions during nanoES. Interestingly, the E_a 's of 60 (+10) and 54 kcal/mol (+11) are similar to the E_a 's measured for the nonspecific ($(\text{scFv} + \mathbf{1}_{\text{ns}})^{n+}$ ions (Table 1), indicating that the binding affinity of the nonspecific ligand in the gas phase is relatively insensitive to the structure of the scFv and CA proteins.

In summary, we have determined for the first time kinetic and energetic data for the dissociation of protein–carbohydrate complexes produced from nonspecific interactions originating during the nanoES process. This study has revealed a number of unexpected results. (1) At the +10 and +11 charge states, the nonspecific ($(\text{scFv} + \mathbf{1}_{\text{ns}})^{n+}$ ions are kinetically more stable than the corresponding ($(\text{scFv} + \mathbf{1}_{\text{sp}})^{n+}$ ions. (2) The nonspecific complex at the +10 charge state is significantly energetically more stable than the corresponding specific complex. (3) The energetic stabilities of the nonspecific ($(\text{scFv} + \mathbf{1}_{\text{ns}})^{n+}$ and $(\text{CA} + \mathbf{1})^{n+}$ ions are similar, suggesting that the nonspecific interactions are insensitive to the structure of protein. The findings of this study have implications for the determination of the affinity and stoichiometry of protein–ligand binding by nanoES-mass spectrometry. They also provide new insight into the intrinsic affinity and specificity of protein–carbohydrate binding.

Acknowledgment. The authors are grateful for financial support provided by NSERC and to D. R. Bundle for generously providing the trisaccharide ligand.

Supporting Information Available: Experimental procedures, nanoES-mass spectra for solutions of scFv and CA with $\mathbf{1}$, BIRD spectra for the ($(\text{scFv} + \mathbf{1})^{n+}$, ($(\text{scFv} + 2(\mathbf{1}))^{n+}$, and $(\text{CA} + \mathbf{1})^{n+}$ ions, kinetic data for the dissociation of the $(\text{CA} + \mathbf{1})^{n+}$ ions (PDF). This material is available free of charge via the Internet at <http://pubs.acs.org>.

References

- (1) (a) Hunter, C. L.; Mauk, A. G.; Douglas, D. J. *Biochemistry* **1997**, *36*, 1018–1025. (b) Wu, Q.; Gao, J.; Joseph-McCarthy, D.; Sigal, G. B.; Bruce, J. E.; Whitesides, G. M.; Smith, R. D. *J. Am. Chem. Soc.* **1997**, *119*, 1157–1158. (c) Rostom, A. A.; Tame, J. R. H.; Ladbury, J. E.; Robinson, C. V. *J. Mol. Biol.* **2000**, *296*, 269–279. (d) van der Kerk-van Hoof, A.; Heck, A. J. R. *J. Mass Spectrom.* **1999**, *34*, 813–819.
- (2) (a) Kitova, E. N.; Bundle, D. R.; Klassen, J. S. *J. Am. Chem. Soc.* **2002**, *124*, 5902–5913. (b) Kitova, E. N.; Bundle, D. R.; Klassen, J. S. *J. Am. Chem. Soc.* **2002**, *124*, 9340–9341. (c) Kitova, E. N.; Wang, W.; Bundle, D. R.; Klassen, J. S. *J. Am. Chem. Soc.* **2002**, *124*, 13980–13981.
- (3) Zdanov, A.; Li, Y.; Bundle, D. R.; Deng, S.-J.; MacKenzie, C. R.; Narang, S. A.; Young, N. M.; Cygler, M. *Proc. Natl. Acad. Sci. U.S.A.* **1994**, *91*, 6423–6427.
- (4) Kitova, E. N.; Klassen, J. S., manuscript in preparation.
- (5) Wang, W.; Kitova, E. N.; Klassen, J. S. *Anal. Chem.* **2003**, *75*, 4945–4955.
- (6) (a) Tholmann, D.; Tonner, D. S.; McMahon, T. B. *J. Phys. Chem.* **1994**, *98*, 2002–2004. (b) Price, W. D.; Schnier, P. D.; Williams, E. R. *Anal. Chem.* **1996**, *68*, 859–866.
- (7) Felitsyn, N.; Kitova, E. N.; Klassen, J. S. *Anal. Chem.* **2001**, *73*, 4647–4661.
- (8) Liu, D.; Wyttenbach, T.; Barran, P. E.; Bowers, M. T. *J. Am. Chem. Soc.* **2003**, *125*, 8458–8464.

JA036998Q